

STATIC ANALYSIS OF EULER-BERNOULLI BEAMS WITH INTERVAL YOUNG'S MODULUS

A. Sofi¹⁾, G. Muscolino²⁾*

¹ *Department of Civil, Energy, Environmental and Materials Engineering, University "Mediterranea" of Reggio Calabria, Via Graziella, Località Feo di Vito, 89124 Reggio Calabria, Italy.*

E-mail: alba.sofi@unirc.it

² *Department of Civil, Building and Environmental Engineering with Information Technology and Applied Mathematics, University of Messina, Villaggio S. Agata, 98166 Messina, Italy. E-mail: gmuscolino@unime.it*

Abstract

A non-probabilistic approach for analyzing the effects of Young's modulus uncertainty on the response of Euler-Bernoulli beams under deterministic static loads is presented. The uncertain material property is described by applying an interval field model based on the so-called *improved interval analysis*. The bounds of the interval response are determined in approximate closed-form by performing a finite difference discretization of the governing interval ordinary differential equation and applying the so-called *Rational Series Expansion*.

The proposed procedure is applied to investigate the effects of Young's modulus uncertainty on the bending response of beams with different boundary conditions.

Keywords: Interval field; Finite difference method; Upper bound and lower bound; Explicit solutions.

1. INTRODUCTION

Over the last decades, many researchers have focused on the development of non-deterministic procedures for assessing structural performance under fluctuations of design parameters. A variety of probabilistic methods, based on the concept of random variables and random fields, has been proposed. As known, a large amount of information is needed to define the probability density function and autocorrelation function characterizing random variables and random fields. When sufficient data are not available, as is commonly the case in early design stage, the credibility of probabilistic predictions may be questionable, especially in the context of reliability analysis.

Non-probabilistic methods, such as convex models, interval models and fuzzy sets (see e.g. [1]) are gaining increasing interest as alternative approaches for handling uncertainties with fragmentary or incomplete information. Among these approaches, the interval model, derived from the interval analysis [2,3], is widely used for incorporating uncertainties in design problems when only the upper and lower bounds of non-deterministic properties are well defined. Several interval-based finite element procedures for the static and dynamic analysis of structures have been developed. For a general overview of the state-of-art and recent advances in interval finite element analysis readers are referred to [4,5]. Recently, the analysis of structures with interval uncertainties under stochastic excitations has also been addressed [6-8].

Two are the main drawbacks commonly faced in the development of interval-based procedures for structural analysis: the drastic overestimation of the interval solution range due to the so-called *dependency phenomenon* [3]; the high computational costs. The *dependency phenomenon* is a consequence of the inability of the *classical* or “*ordinary*” interval arithmetic to keep track of the dependency between interval variables. Indeed, it occurs when an expression contains multiple instances of one or more interval variables and often leads to useless results for structural design purposes. In the literature, several approaches have been introduced to limit the effects of the *dependency phenomenon*, such as: the *generalized interval arithmetic* [9], the *affine arithmetic*

[10,11], the *parameterized interval analysis* [12] and the *improved interval analysis (IIA)* [7,8]. The high computational costs are inherent in any non-deterministic approach either probabilistic or non-probabilistic. The challenging task is to build efficient procedures alternative to the repeated deterministic analyses needed in principle to predict the effects of uncertainties on the structural response. Within the interval framework, researchers focus their effort on obtaining a good compromise between tight enclosures of the solution and low computational costs.

Another crucial issue is the need to account for the spatial character of uncertainties like material properties or load distributions. Probabilistic methods handle the spatial dependency of non-deterministic properties by using the well-established concept of random field (see e.g. [13]). Conversely, taking into account the spatial variability of uncertainties within the same realization of a model is still a main challenge in a non-probabilistic context. Indeed, the inability of the *classical interval analysis (CIA)* to describe the spatial dependency of interval properties within a given domain is one of the main drawbacks of interval finite element (IFE) procedures which commonly assign an interval variable to each FE. This approach relies on the extreme assumption of spatial independency of the uncertain properties which is both unrealistic and computationally onerous. Alternatively, a single interval variable over the entire model can be assumed which implies the introduction of the opposite extreme hypothesis of total spatial dependency. In an effort to provide a more realistic description of spatially variable interval uncertainties, the so-called *interval field* [14,15] has been introduced as a natural extension of the random field concept. Explicit and implicit interval fields [16] have been defined to represent dependent uncertainties arising both in the model definition phase and in the post-processing phase of a static FE analysis. Basically, the explicit interval field model describes a spatially dependent interval parameter as superposition of a limited number of reference patterns, say basis vectors, and interval factors. The reference patterns are defined based on expert knowledge of the modeled system. This concept has been recently extended by the authors [17] who proposed a novel interval field model of input uncertain parameters based on the *IIA* and the related *extra unitary interval (EUI)*. The underlying idea is to account for the

dependency between interval values of a non-deterministic property at various locations by introducing a deterministic symmetric non-negative bounded function playing the same role of the autocorrelation function in random field theory.

This paper presents a non-probabilistic procedure for analyzing the response of Euler-Bernoulli beams with uncertain-but-bounded Young's modulus subjected to deterministic static loads. The problem of the propagation of material uncertainties to the bending response of beams is a topic of great interest which is commonly tackled in the literature by applying probabilistic methods. Accordingly, the spatially variable uncertain material property is modelled as a random field with assigned autocorrelation function and the probabilistic characterization of the response random field is performed (see e.g. [18-21]). In the present paper, two key issues are addressed: *i*) the description of the spatial character of the uncertain material property within the interval framework; *ii*) the limitation of the overestimation of the interval solution range affecting the *CIA*. To cope with the first issue, the spatial variability of the uncertain Young's modulus along the Euler-Bernoulli beam is here described by applying the interval field model based on the *IIA* recently proposed by the authors [17]. By exploiting the main properties of the *IIA*, a meaningful analogy between the interval and random field concept is established which suggests to apply a Karhunen-Loève (KL)-like decomposition of the Young's modulus interval field. Then, performing a finite difference (FD) discretization of the fourth-order ordinary interval differential equation governing the equilibrium of the Euler-Bernoulli beam, approximate closed-form expressions of the lower bound (LB) and upper bound (UB) of the interval displacement field are derived. This remarkable result is achieved by combining the *IIA* with the so-called *Rational Series Expansion (RSE)* recently proposed by the authors [8,22] for evaluating the inverse of an interval matrix with small rank-*r* modifications. Both the consistency of the interval field model and the accuracy of the proposed estimates of the response bounds are demonstrated through numerical results.

The paper is organized as follows: in the next section, the fundamentals of the *IIA* are briefly outlined; Section 3 is devoted to the definition of the interval field model based on the *IIA*, recently proposed by Muscolino et al. [17] for describing the spatial dependency of uncertain-but-bounded properties; in Section 4, the problem of an Euler-Bernoulli beam with interval Young's modulus is formulated and an efficient procedure for deriving approximate explicit expressions of the bounds of the interval displacement field is presented; finally, for validation purposes, numerical results concerning both statically determinate and indeterminate beams with interval Young's modulus under a deterministic uniformly distributed load are reported in Section 5.

2. IMPROVED INTERVAL ANALYSIS (IIA) BASED ON THE EXTRA UNITARY INTERVAL (EUI)

The interval model of uncertainty has been originally developed from the *classical interval analysis (CIA)* [3] which, unlike classical arithmetic, deals with intervals of real numbers. The key idea is to treat the uncertain parameters ever present in structural engineering problems as interval numbers with given lower bound (LB) and upper bound (UB). An interval variable is denoted by $\alpha^I \triangleq [\underline{\alpha}, \bar{\alpha}] \in \mathbb{IR}$ such that $\underline{\alpha} \leq \alpha \leq \bar{\alpha}$, \mathbb{IR} being the set of all real interval numbers. The symbols $\underline{\alpha}$ and $\bar{\alpha}$ denote the LB and UB of the interval, respectively, while the apex *I* characterizes the interval variables. Unlike the widely used probabilistic approach, the interval model allows to handle uncertainties based on limited information, say their range of variability, without requiring the knowledge of the type of distribution within such range. The response of structural systems with interval uncertainties turns out to have an interval nature. In other words, the response does not take a given value but it varies within a complicated region and the aim of the interval structural analysis is to evaluate the maximum and minimum values of the response. To cope with such a hard task, the hypercubic approximation is commonly adopted [5].

Despite the simplicity of the interval model of uncertainty, its application to real engineering problems often leads to serious shortcomings. The main limitation is the so-called *dependency phenomenon* [3] which arises when an expression contains multiple instances of one or more interval variables due to the inability of the *CIA* to keep track of the dependency between interval variables. Such phenomenon introduces a high amount of conservatism leading to useless results for real sized structures. In the literature, several approaches have been introduced in an attempt to limit the overestimation of the interval solution width caused by the *dependency phenomenon*, such as: the *generalized interval arithmetic* [9], the *affine arithmetic* [10,11], the *parameterized interval analysis* [12] and the *improved interval analysis (IIA)* [7,8].

The aim of this section is to present the fundamentals of the *IIA* developed by the authors [7,8] in the framework of structural analysis following the philosophy of the *affine arithmetic* [10,11]. The essence of the *IIA* can be identified with the introduction of the so-called *extra unitary interval (EUI)*, $\hat{e}_i^l \triangleq [-1, +1]$, defined in such a way that the following properties hold:

$$\begin{aligned}
\hat{e}_i^l - \hat{e}_i^l &= [0, 0]; & \hat{e}_i^l \times \hat{e}_i^l &= (\hat{e}_i^l)^2 = [1, 1]; \\
\hat{e}_i^l \times \hat{e}_j^l &= \hat{e}_{ij}^l = [-1, +1], & i &\neq j; \\
\hat{e}_i^l / \hat{e}_i^l &= [1, 1]; & x_i \hat{e}_i^l \pm y_i \hat{e}_i^l &= (x_i \pm y_i) \hat{e}_i^l; \\
x_i \hat{e}_i^l \times y_i \hat{e}_i^l &= x_i y_i (\hat{e}_i^l)^2 = x_i y_i [1, 1].
\end{aligned} \tag{1a-f}$$

where the subscript i indicates that the *EUI* is associated to the i -th uncertain-but-bounded parameter. In the previous equations, $[1, 1] = 1$ denotes the so-called unitary *thin interval*. It is recalled that a thin interval occurs when $\underline{\alpha} = \bar{\alpha}$ and it is defined as $\alpha^l \triangleq [\underline{\alpha}, \underline{\alpha}]$, so that $\alpha \in \mathbb{R}$.

Notice that the *EUI*, $\hat{e}_i^l \triangleq [-1, +1]$, differs from the *classical unitary interval (CUI)*, $e^l \triangleq [-1, +1]$, which follows the rules of the *CIA*, leading to the following properties:

$$\begin{aligned}
e^l - e^l &= [-2, +2]; & e^l \times e^l &= [-1, +1]; \\
e^l / e^l &\text{ does not exist because } 0 \in [-1, +1]; \\
x_i e^l \pm y_i e^l &= [-x_i - y_i, x_i + y_i]; \\
x_i e^l \times y_i e^l &= [-x_i y_i, x_i y_i].
\end{aligned} \tag{2a-e}$$

A remarkable difference between the *EUI*, $\hat{e}_i^l \triangleq [-1, +1]$, and the *CUI*, $e^l \triangleq [-1, +1]$, is that the first one is associated to the i -th uncertain-but-bounded parameter. This allows to keep track of the dependencies between interval variables throughout calculations thus limiting the overestimation due to the *dependency phenomenon*. Furthermore, the use of the *EUI* enables to eliminate some physically inconsistent results of the *CIA* such as the subcancellation property (see Eq. (2a)).

The *IIA* expresses the i -th interval variable $\alpha_i^l \triangleq [\underline{\alpha}_i, \bar{\alpha}_i] \in \mathbb{IR}$ in the so-called *affine form*, i.e.:

$$\alpha_i^l = \alpha_{0,i} + \Delta\alpha_i \hat{e}_i^l \tag{3}$$

where \hat{e}_i^l is the *EUI* associated to α_i^l (see Eq. (1a-f)) and

$$\alpha_{0,i} = \frac{1}{2}(\underline{\alpha}_i + \bar{\alpha}_i); \quad \Delta\alpha_i = \frac{1}{2}(\bar{\alpha}_i - \underline{\alpha}_i) \tag{4a,b}$$

denote the midpoint and the deviation amplitude of α_i^l , respectively.

The *IIA* has been applied by the authors to handle uncertainties arising in quite different structural problems such as randomly excited linear structures [7,8] or one-dimensional non-local heterogeneous continua [17]. Numerical results have demonstrated that the *IIA* enables to drastically reduce the effects of the *dependency phenomenon*. In the present paper, the main properties of the *IIA* are exploited to handle the spatial dependency of interval uncertainties in structural engineering problems.

3. SPATIAL DEPENDENCY OF INTERVAL UNCERTAINTIES

3.1 Interval field model based on the *IIA*

Interval variables fail to describe spatially varying uncertainties since they do not allow to quantify any sort of dependency between adjacent values of an uncertain property within a given domain. To cope with this problem, Moens et al. [14] introduced the so-called *interval field* as a natural extension of the random field concept. An interval field is conceived as being able to define a form of dependency between adjacent interval values of an uncertain property that cannot differ as much as values that are further apart.

In this section, the main features of a novel interval field model based on the *IIA* and the related *EUI* are presented [17]. Without loss of generality, attention is focused on the variability of a structural parameter, such as the Young's modulus of the material, within the 1D domain $0 \leq x \leq L$ which commonly occurs, for instance, in beam problems. It is assumed that the uncertain elastic modulus is represented by the following interval function:

$$E^I(x) = [\underline{E}(x), \bar{E}(x)] \quad (5)$$

where $\underline{E}(x)$ and $\bar{E}(x)$ denote the LB and UB for every $x \in \mathbb{R}$ within the domain $[0, L]$. In other words, it is assumed that each realization of the uncertain Young's modulus may vary arbitrarily within the region enclosed by the LB and UB, $\underline{E}(x)$ and $\bar{E}(x)$, as sketched in Fig.1 where for the sake of simplicity the bounds are assumed constant.

Let $B^I(x) = [\underline{B}(x), \bar{B}(x)]$ denote a dimensionless interval function having zero midpoint and deviation amplitude $\Delta B(x) < 1$. Then, without loss of generality, the interval function $E^I(x)$ can be defined as follows:

$$E^I(x) = E_0 [1 + B^I(x)], \quad x \in [0, L] \quad (6)$$

with midpoint value $E_0 \in \mathbb{R}$, taken constant over the whole domain $[0, L]$, and deviation amplitude $\Delta E(x)$ given, respectively, by

$$\begin{aligned} \text{mid}\{E^I(x)\} &= \frac{\bar{E}(x) + \underline{E}(x)}{2} \equiv E_0; \\ \Delta E(x) &= \frac{\bar{E}(x) - \underline{E}(x)}{2} \equiv E_0 \Delta B(x), \quad x \in [0, L]. \end{aligned} \tag{7a,b}$$

In Eq. (7a), $\text{mid}\{\bullet\}$ denotes the midpoint of the interval quantity into curly parentheses. Furthermore, according to Eq. (6), the midpoint value coincides with the nominal value of the uncertain material property.

The key issue is to assume an appropriate pattern for modelling the spatial dependency of the interval function $B^I(x)$ which in turn reflects the dependency between values of the interval field $E^I(x)$ at different locations. Such spatial dependency is assumed to be governed by a real deterministic symmetric non-negative function, $\Gamma_B(x, \xi)$, defined as follows:

$$\Gamma_B(x, \xi) = \text{mid}\{B^I(x)B^I(\xi)\} \equiv \frac{\text{mid}\{E^I(x)E^I(\xi)\}}{(E_0)^2} - 1, \quad x, \xi \in [0, L]. \tag{8}$$

Notice that $\Gamma_B(x, \xi)$ represents the midpoint of the dimensionless interval function $B^I(x)B^I(\xi)$ which is related to the midpoint of the interval function $E^I(x)E^I(\xi)$ by Eq. (8). The function $\Gamma_B(x, \xi)$ is herein named *spatial dependency function*.

If the midpoint operator, $\text{mid}\{\bullet\}$, is viewed as the equivalent of the stochastic average operator, it may be stated that within the interval framework the function $\Gamma_B(x, \xi)$ plays the same role of the autocorrelation function characterizing probabilistically a random field. Based on this analogy, a Karhunen-Loève (KL)-like decomposition [23] can be applied, i.e.:

$$\Gamma_B(x, \xi) = \sum_{i=1}^{\infty} \lambda_i \psi_i(x) \psi_i(\xi) \Rightarrow \Gamma_B(x, x) \equiv \text{mid} \left\{ \left(B^I(x) \right)^2 \right\} = \sum_{i=1}^{\infty} \lambda_i \psi_i^2(x) \quad (9)$$

where λ_i , ($i=1,2,\dots$), is the i -th *eigenvalue* of the bounded symmetric non-negative function, $\Gamma_B(x, \xi)$, and $\psi_i(x)$ ($i=1,2,\dots$) is the corresponding *eigenfunction*, solutions of the following homogeneous Fredholm integral equation of the second kind:

$$\int_0^L \Gamma_B(x, \xi) \psi_i(x) dx = \lambda_i \psi_i(\xi). \quad (10)$$

The eigenvalues, λ_i , are real positive numbers and the associated eigenfunctions, $\psi_i(x)$, are real functions satisfying the following orthogonality condition:

$$\int_0^L \psi_i(x) \psi_j(x) dx = \begin{cases} 1 & \text{if } i = j \\ 0 & \text{if } i \neq j. \end{cases} \quad (11)$$

The expansion in Eq. (9) is usually truncated to the first N terms to reduce the computational burden of the subsequent structural analysis.

Taking into account the definition (8) of the function $\Gamma_B(x, \xi)$ and the decomposition (9) truncated to the first N terms, the following expression of the dimensionless interval function $B^I(x)$ is readily found:

$$B^I(x) = \sum_{i=1}^N \sqrt{\lambda_i} \psi_i(x) \hat{e}_i^I, \quad x \in [0, L]. \quad (12)$$

Indeed, replacing Eq. (12) into Eq. (8) and exploiting the properties (1b,c) of the *EUI*, \hat{e}_i^I , yields exactly the same expression of the function $\Gamma_B(x, \xi)$ given by Eq. (9). Notice that Eq. (12) provides the dimensionless interval function $B^I(x)$ as linear combination of deterministic functions $\sqrt{\lambda_i} \psi_i(x)$ and *EUIs* \hat{e}_i^I ($i=1,2,\dots,N$). This remarkable result cannot be obtained by applying the

CIA since the product between interval functions $B^I(x)B^I(\xi)$ in Eq. (8) provides a quite different result, i.e.:

$$B^I(x)B^I(\xi) = \left[\min(\underline{B}(x)\underline{B}(\xi), \underline{B}(x)\bar{B}(\xi), \bar{B}(x)\underline{B}(\xi), \bar{B}(x)\bar{B}(\xi)), \max(\underline{B}(x)\underline{B}(\xi), \underline{B}(x)\bar{B}(\xi), \bar{B}(x)\underline{B}(\xi), \bar{B}(x)\bar{B}(\xi)) \right]. \quad (13)$$

This implies that the definition (12) of the dimensionless interval function $B^I(x)$ does not hold in the context of the *CIA*.

Substituting Eq. (12) into Eq.(6), the interval field $E^I(x)$ can be recast as:

$$E^I(x) = E_0 \left[1 + \sum_{i=1}^N \sqrt{\lambda_i} \psi_i(x) \hat{e}_i^I \right], \quad x \in [0, L] \quad (14)$$

where \hat{e}_i^I is the i -th *EUI*. Then, the LB and UB, $\underline{E}(x)$ and $\bar{E}(x)$, of the interval Young's modulus $E^I(x)$ in Eq. (14) can be defined as:

$$\underline{E}(x) = E_0 [1 - \Delta B(x)]; \quad \bar{E}(x) = E_0 [1 + \Delta B(x)], \quad x \in [0, L] \quad (15a,b)$$

where

$$\Delta B(x) = \frac{\Delta E(x)}{E_0} = \sum_{i=1}^N \left| \sqrt{\lambda_i} \psi_i(x) \right|, \quad x \in [0, L] \quad (16)$$

with $|\bullet|$ denoting the absolute value of \bullet .

3.2 Interval field as non-probabilistic counterpart of random field

Though the interval field (14) is formally analogous to the model proposed by Verhaeghe et al. [15], it is conceptually different. The main difference consists in the use of the *IIA* and the related *EUI*, \hat{e}_i^I , which allows to give a meaningful interpretation of the function $\Gamma_B(x, \xi)$ as the non-

probabilistic counterpart of the autocorrelation function in random field theory. Such interpretation suggests to build the interval field model by analogy with the random field definition [17]. To gain further insight into this concept, let us assume now that the uncertain Young's modulus is modelled as a homogeneous Gaussian random field, defined as:

$$\tilde{E}(x) = E_0 [1 + \tilde{B}(x)], \quad x \in [0, L] \quad (17)$$

where $\tilde{B}(x)$ is a homogeneous zero-mean Gaussian random field describing the dimensionless fluctuation of the elastic modulus about the nominal or mean-value, $E_0 = E\langle \tilde{E}(x) \rangle$, $E\langle \bullet \rangle$ being the mathematical expectation operator. In order to guarantee positive values of $\tilde{E}(x)$, the random field $\tilde{B}(x)$ must satisfy the restriction $|\tilde{B}(x)| < 1$. Notice that, such a condition is not mathematically satisfied for Gaussian random fields unless small fluctuations are considered. The zero-mean random field $\tilde{B}(x)$ is completely characterized from a probabilistic point of view by the autocorrelation function:

$$R_{\tilde{B}\tilde{B}}(x, \xi) = E\langle \tilde{B}(x)\tilde{B}(\xi) \rangle. \quad (18)$$

By comparing Eqs. (17) and (18) with Eqs. (6) and (8), respectively, the analogy between the midpoint operator, $\text{mid}\{\bullet\}$, and the stochastic average operator, $E\langle \bullet \rangle$, can be naturally established and the real deterministic symmetric non-negative function, $\Gamma_B(x, \xi)$, can be consistently viewed as the non-probabilistic counterpart of the autocorrelation function.

3.3 Limit cases: total spatial dependency and spatial independency of uncertainties

The interval field may be viewed as an intermediate model of uncertainty between two extreme approaches commonly used within a non-probabilistic context. Such approaches rely on the basic assumption that the uncertain parameters exhibit either total spatial dependency or spatial

independency. In the first case, an uncertain parameter can be represented as a single interval variable constant over the whole domain. Conversely, spatially independent uncertainties can be handled by introducing an interval variable for each element of a finite element (FE) model or of a discretized system. Obviously, both the aforementioned approaches are unrealistic and a more reliable description is generally obtained assuming that the values of an uncertain property at different locations depend on each other to some extent, according to the interval field concept. An interesting feature of the interval field based on the *IIA* to be investigated is the capability of describing total spatially dependent and spatially independent uncertainties as limit cases. To this aim, without loss of generality, it is here assumed that the real deterministic symmetric non-negative function, $\Gamma_B(x, \xi)$, governing the spatial dependency of the interval field $E^I(x)$ has the following exponential form:

$$\Gamma_B(x, \xi) = C_B^2 \exp\left(-\frac{|x - \xi|}{l_B}\right) \quad (19)$$

where C_B and l_B are appropriate parameters to be set based on the available information on the uncertain property. Specifically, the parameter C_B affects the deviation amplitude of the interval field and thus the uncertainty level, while the value of l_B rules the spatial dependency of the uncertain Young's modulus. In this connection, C_B and l_B may be regarded, respectively, as the non-probabilistic counterpart of the standard deviation and correlation length in random field theory. Indeed, based on Eq.(19), it can be seen that as l_B decreases, the interval Young's modulus $E^I(x)$ at a given position x depends only on the values $E^I(\xi)$ at close locations ξ . In the limit, as $l_B \rightarrow 0$ the uncertain material property becomes spatially independent and the proposed interval field model ideally reduces to a series of independent interval variables, one for each abscissa within the domain $[0, L]$. On the other extreme, if $l_B \rightarrow \infty$, the exponential function in Eq. (19) approaches the value C_B^2 . This implies that the dimensionless interval function $B^I(x)$ describing

the zero-midpoint fluctuation of the interval Young's modulus with respect to its nominal value (see Eq. (6)) reduces to a symmetric interval variable, i.e.:

$$B^I(x) \equiv b^I = b\hat{e}^I \quad (20)$$

whose radius b can be evaluated from Eq.(8) taking into account that $\Gamma_B(x, \xi) \rightarrow C_B^2$:

$$\Gamma_B(x, \xi) = \text{mid}\{B^I(x)B^I(\xi)\} = b^2 = C_B^2 \Rightarrow b = C_B \quad (21)$$

being $\hat{e}^I \times \hat{e}^I = [1,1]$ (see Eq. (1b)). Physically, this circumstance corresponds to the total spatial dependency condition in which the uncertain Young's modulus is described by a single interval variable constant over the whole domain $[0, L]$, i.e.:

$$E^I = E_0(1 + b\hat{e}^I), \quad x \in [0, L]. \quad (22)$$

The bounds of the interval Young's modulus E^I clearly correspond to the bounds of the *EUI*, \hat{e}^I , i.e.:

$$\underline{E} = E_0(1 - b); \quad \bar{E} = E_0(1 + b). \quad (23a,b)$$

4. EULER-BERNOULLI BEAM WITH INTERVAL YOUNG'S MODULUS

4.1 Interval differential equilibrium equation

Let us now consider a linear elastic Euler-Bernoulli beam under a deterministic transversally distributed load $p_z(x)$ with uncertain Young's modulus of the material, $E^I(x)$, modelled as an interval field according to the definition presented in the previous section (see Fig. 2).

The transverse displacement of the beam is described by an interval field $w^I(x)$ ruled by the following fourth-order ordinary interval differential equation:

$$\frac{d^2}{dx^2} \left[E^I(x) J(x) \frac{d^2 w^I(x)}{dx^2} \right] = p_z(x) \quad (24)$$

where $J(x)$ denotes the moment of inertia of the beam cross-section. Equation (24) must be supplemented by the pertinent kinematic and static boundary conditions, herein assumed deterministic, i.e. independent of interval variables. Substituting the expression (14) of the interval Young's modulus $E^I(x)$, Eq. (24) reads:

$$E_0 \frac{d^2}{dx^2} \left[J(x) \frac{d^2 w^I(x)}{dx^2} \right] + E_0 \sum_{i=1}^N \sqrt{\lambda_i} \hat{e}_i^I \frac{d^2}{dx^2} \left[\psi_i(x) J(x) \frac{d^2 w^I(x)}{dx^2} \right] = p_z(x) \quad (25)$$

which differs from the equilibrium equation of the beam with nominal value of the modulus of elasticity, E_0 , just for the second term on the left-hand side.

Within the interval framework, the solution of Eq. (25) consists in finding the narrowest interval containing all possible transverse displacement fields, $w(x)$, corresponding to all realizations of the interval Young's modulus $E^I(x)$ between its bounds (see Eqs. (15a,b)). Within the context of the *IIA*, in this study a procedure for deriving approximate closed-form expressions of the bounds of the interval displacement field $w^I(x)$ is presented. The first step of the procedure involves the finite difference (FD) discretization of the governing equation. Then, let us subdivide the beam domain $[0, L]$ into n intervals Δx , so that $x_j = j\Delta x$ is the abscissa of the j -th grid point with $j=0,1,2,\dots,n$. Introducing the standard finite difference approximation of second-order derivative, the following discretized version of the equilibrium equation (25) is obtained:

$$E_0 J_{j-1} w_{j-2}^I - 2E_0 (J_{j-1} + J_j) w_{j-1}^I + E_0 (J_{j-1} + 4J_j + J_{j+1}) w_j^I - 2E_0 (J_j + J_{j+1}) w_{j+1}^I + E_0 J_{j+1} w_{j+2}^I + \sum_{i=1}^N \left[s_{j-1}^{(i)} w_{j-2}^I - 2(s_{j-1}^{(i)} + s_j^{(i)}) w_{j-1}^I + (s_{j-1}^{(i)} + 4s_j^{(i)} + s_{j+1}^{(i)}) w_j^I - 2(s_j^{(i)} + s_{j+1}^{(i)}) w_{j+1}^I + s_{j+1}^{(i)} w_{j+2}^I \right] \hat{e}_i^I = F_j \quad (26)$$

where

$$\begin{aligned}
w_j^I &= w^I(x_j) = w^I(j\Delta x); \\
J_j &= J(x_j) = J(j\Delta x); \\
F_j &= p_z \Delta x^4 = p_z(x_j) \Delta x^4 = p_z(j\Delta x) \Delta x^4; \\
s_j^{(i)} &= E_0 J_j \sqrt{\lambda_i} \psi_{ij} = E_0 J(x_j) \sqrt{\lambda_i} \psi_i(x_j) = E_0 J(j\Delta x) \sqrt{\lambda_i} \psi_i(j\Delta x).
\end{aligned} \tag{27a-d}$$

Equation (26) represents a set of linear interval equations which can be recast in the following compact form:

$$\mathbf{K}^I \mathbf{w}^I = (\mathbf{K}_0 + \Delta \mathbf{K}_B^I) \mathbf{w}^I = \mathbf{F} \tag{28}$$

where \mathbf{w}^I is the vector of order m collecting the unknown interval displacements w_j^I at the grid points whose order m can be determined once the boundary conditions are imposed; \mathbf{F} is the m -vector listing the forces at the grid points F_j (see Eq. (27c)). The $(m \times m)$ interval coefficient matrix \mathbf{K}^I in Eq. (28) is sum of two terms: the first one is the coefficient matrix \mathbf{K}_0 pertaining to the elastic beam with nominal Young's modulus, E_0 , constant over the whole domain $[0, L]$; the second term is the interval matrix $\Delta \mathbf{K}_B^I$ accounting for the uncertain nature of the elastic modulus, which can be expressed as superposition of N deterministic matrices, $\Delta \mathbf{K}_{B,i}$, multiplied by the corresponding *EUIs*, i.e.:

$$\Delta \mathbf{K}_B^I = \sum_{i=1}^N \Delta \mathbf{K}_{B,i} \hat{e}_i^I. \tag{29}$$

4.2 Bounds of the interval displacement field

Once the set of linear interval equations governing the interval displacements at the grid points w_j^I has been determined, the aim of the analysis is to determine the narrowest interval \mathbf{w}^I containing all possible vectors \mathbf{w} satisfying Eq.(28), when the matrices $\Delta \mathbf{K}_{B,i} \hat{e}_i^I$ assume all possible values within the intervals $[-\Delta \mathbf{K}_{B,i}, +\Delta \mathbf{K}_{B,i}]$, ($i = 1, 2, \dots, N$). It is worth remarking that the square interval

matrix \mathbf{K}^I is regular, that is each matrix $\mathbf{K} \in \mathbf{K}^I$ is non-singular (Rohn, 1990), so that the solution \mathbf{w}^I of Eq.(28), exists for all $\mathbf{K} \in \mathbf{K}^I$ and can be formally written as

$$\mathbf{w}^I = (\mathbf{K}^I)^{-1} = (\mathbf{K}_0 + \Delta\mathbf{K}_B^I)^{-1} \mathbf{F} = \left(\mathbf{K}_0 + \sum_{i=1}^N \Delta\mathbf{K}_{B,i} \hat{e}_i^I \right)^{-1} \mathbf{F}. \quad (30)$$

Under the assumption of small dimensionless deviation amplitude of the interval elastic modulus, i.e. $\Delta B(x) \ll 1$ for all $x \in [0, L]$ (see Eq. (16)), the interval vector \mathbf{w}^I is herein derived in approximate closed-form by applying the so-called *Rational Series Expansion (RSE)*, recently proposed by the authors [8,22] as an alternative explicit expression of the Neumann series [23,25,26] for evaluating the inverse of a matrix with small rank- r modifications. The starting point to apply the *RSE* is the decomposition by columns of the matrix $\Delta\mathbf{K}_{B,i}$ in Eq. (29) which leads to the following expression of the interval coefficient matrix \mathbf{K}^I :

$$\mathbf{K}^I = \mathbf{K}_0 + \Delta\mathbf{K}_B^I = \mathbf{K}_0 + \sum_{i=1}^N \sum_{\ell=1}^m \mathbf{k}_{B,i\ell} \mathbf{v}_\ell^T \hat{e}_i^I \quad (31)$$

where $\mathbf{k}_{B,i\ell}$ is the ℓ -th column of the matrix $\Delta\mathbf{K}_{B,i}$ and \mathbf{v}_ℓ is a column vector of order m containing all zeros except the ℓ -th element which is equal to 1. By applying the *RSE*, the approximate inverse of the interval matrix in Eq.(31) takes the following explicit form:

$$(\mathbf{K}^I)^{-1} = (\mathbf{K}_0 + \Delta\mathbf{K}_B^I)^{-1} \approx \mathbf{K}_0^{-1} - \sum_{i=1}^N \sum_{\ell=1}^m \frac{\hat{e}_i^I}{1 + \hat{e}_i^I d_{B,i\ell}} \mathbf{D}_{B,i\ell} \quad (32)$$

where

$$d_{B,i\ell} = \left| \mathbf{v}_\ell^T \mathbf{K}_0^{-1} \mathbf{k}_{B,i\ell} \right|; \quad \mathbf{D}_{B,i\ell} = \mathbf{K}_0^{-1} \mathbf{k}_{B,i\ell} \mathbf{v}_\ell^T \mathbf{K}_0^{-1}. \quad (33a,b)$$

It is worth mentioning that the *RSE* of the inverse of the interval coefficient matrix \mathbf{K}^I in Eq. (32) holds if and only if the condition $d_{B,i\ell} < 1$ is satisfied.

Upon rewriting the ratio appearing in the summation in Eq. (32) in *affine form* and replacing the resulting expression of the inverse matrix $(\mathbf{K}^I)^{-1}$ into Eq. (30), the interval displacement vector $\mathbf{w}^I \in \mathbb{IR}^m$ can be recast as follows:

$$\mathbf{w}^I \approx \left[\mathbf{K}_0^{-1} + \sum_{i=1}^N \sum_{\ell=1}^m (a_{0,i\ell} + \Delta a_{i\ell} \hat{e}_i^I) \mathbf{D}_{B,i\ell} \right] \mathbf{F}. \quad (34)$$

In the previous equation, $a_{0,i\ell}$ and $\Delta a_{i\ell}$ denote the midpoint and deviation amplitude of the generic series term $\hat{e}_i^I / (1 + \hat{e}_i^I d_{B,i\ell})$ in Eq. (32), which after some interval algebra, can be written as:

$$a_{0,i\ell} = \frac{d_{B,i\ell}}{1 - d_{B,i\ell}^2}; \quad \Delta a_{i\ell} = \frac{1}{1 - d_{B,i\ell}^2}. \quad (35a,b)$$

Based on the closed-form solution in Eq. (34) and following the *IIA*, the LB and UB, $\underline{\mathbf{w}}$ and $\bar{\mathbf{w}}$, of the interval response vector \mathbf{w}^I can be evaluated as follows:

$$\underline{\mathbf{w}} = \mathbf{w}_0 - \Delta \mathbf{w}; \quad \bar{\mathbf{w}} = \mathbf{w}_0 + \Delta \mathbf{w} \quad (36a,b)$$

where

$$\mathbf{w}_0 = \left(\mathbf{K}_0^{-1} + \sum_{i=1}^N \sum_{\ell=1}^m a_{0,i\ell} \mathbf{D}_{B,i\ell} \right) \mathbf{F}; \quad \Delta \mathbf{w} = \sum_{i=1}^N \left| \sum_{\ell=1}^m \Delta a_{i\ell} \mathbf{D}_{B,i\ell} \mathbf{F} \right| \quad (37a,b)$$

are the midpoint and the deviation amplitude of the interval displacement vector \mathbf{w}^I , while the symbol $|\bullet|$ in Eq. (37b) denotes the component wise absolute value.

5. NUMERICAL APPLICATIONS

Extensive numerical studies have been carried out to validate the non-probabilistic approach presented in the paper. In this section, some representative numerical results are reported. The section is organized as follows. First, the main features of the interval field model (see Eq. (14)) adopted to represent the uncertain elastic modulus $E^I(x)$ are scrutinized. To this aim, an

exponential *spatial dependency function*, $\Gamma_B(x, \xi)$, is assumed (see Eq.(19)) and the midpoint value of the Young's modulus is set to $E_0 = 30$ GPa. Different values of the parameters l_B and C_B governing, respectively, the spatial dependency and the deviation amplitude of the interval field are considered. The eigenvalues, λ_i , and eigenfunctions, $\psi_i(x)$, of the exponential *spatial dependency function* are evaluated as outlined in Appendix. Then, attention is focused on the effects of Young's modulus uncertainty on the interval displacement field of both statically determined and indeterminate Euler-Bernoulli beams. Specifically, two different boundary conditions are considered: simply supported (see Fig. 5) and fixed-simply supported (see Fig. 10). In both cases, the beam is assumed to carry a deterministic uniformly distributed load of intensity p_z per unit length. The geometrical properties of the beam are selected as follows: span-length $L = 24$ m and rectangular cross-section with $b = 0.5$ m and $h = 1.6$ m (see Figs. 5 and 10). The interval ordinary differential equation (24) governing the response of the beam is discretized by the FDM using a uniform grid with $n = 240$ subdivisions. More refined grids do not provide appreciable improvement of the accuracy.

5.1 Interval field with exponential *spatial dependency function*

Figures 3a,b display the bounds of the interval Young's modulus $E^I(x)$ evaluated according to Eqs. (15a,b) for different values of the parameters l_B and C_B versus the dimensionless abscissa x/L , with $x \in [0, L]$. The midpoint E_0 is also reported for completeness. For any choice of the parameters l_B and C_B , the exponential *spatial dependency function*, $\Gamma_B(x, \xi)$, is decomposed by applying Eq. (9) truncated to the first $N = 24$ terms with the eigenvalues, λ_i , and eigenfunctions, $\psi_i(x)$, evaluated as outlined in Appendix. In Fig. 3a, the bounds of the interval Young's modulus $E^I(x)$ corresponding to $C_B = 0.05$ and three different values of the parameter l_B are plotted. Notice that the region of the uncertain material property becomes wider as l_B decreases. Figure 3b

shows that, for a given value of the parameter l_B , say $l_B = 0.5L$, the Young's modulus region widens to a larger extent as the coefficient C_B increases. Indeed, the deviation amplitude of the proposed interval field model, $\Delta E(x)$, with exponential *spatial dependency function* (19), turns out to depend linearly on C_B (see Eqs. (16) and (A.3)).

To gain further insight into the influence of the parameter l_B on the interval field, Figs. 4a,b show the UB and LB of the interval Young's modulus field $E^I(x)$ along with the samples $E^{(r)}(x)$ ($r = 1, 2, \dots, 2^N$) pertaining to all possible combinations of the bounds of the EUIs \hat{e}_i^I ($i = 1, 2, \dots, N$) in Eq.(14) for two different values of l_B , say $l_B = 0.5L$ and $l_B = 2L$. For the sake of clarity, only the first $N = 4$ terms are retained in the decomposition (9) of the function $\Gamma_B(x, \xi)$ so that the number of samples of the interval field is $2^N = 16$. As expected, the bounds of the interval Young's modulus field, $\underline{E}(x)$ and $\bar{E}(x)$, turn out to be the envelopes of the $2^N = 16$ samples. Furthermore, it can be observed that the samples $E^{(r)}(x)$ are significantly affected by the parameter l_B . Specifically, as shown in Fig. 4b, an increase of the parameter l_B implies that the pattern of the samples $E^{(r)}(x)$ becomes more uniform over the spatial domain since the value of the uncertain material property at a given abscissa x depends on the values it takes at different abscissas ξ within a larger distance from x . As outlined in Section 3.3, when $l_B \rightarrow \infty$, the total spatial dependency condition is recovered and the interval field reduces to an interval variable constant over the whole domain (see Eq.(22)). Conversely, Fig. 4a shows that, as smaller values of the parameter l_B are considered, the pattern of the samples becomes more irregular since the value of the interval field at a given abscissa x depends only on the values it takes at different locations ξ close to x . In the limit, as $l_B \rightarrow 0$ the interval field ideally reduces to a set of independent interval variables one at each abscissa $x \in [0, L]$. The results reported in Figs. 4a,b demonstrate the

capability of the proposed interval field model of describing the uncertain material property under the extreme assumptions of total spatial dependency and total spatial independency.

5.2 Simply supported beam with interval Young's modulus

Consider the simply supported beam under a deterministic uniformly distributed load p_z shown in Fig. 5.

Let the uncertain Young's modulus of the material be described by the interval field $E^I(x)$ with exponential *spatial dependency function* $\Gamma_B(x, \xi)$ characterized in the previous sub-section. The main purpose of numerical simulations is to analyze the effects of the uncertain elastic modulus on the interval displacement field $w^I(x)$ by applying the procedure described in Section 4. To this aim, as a first step, the accuracy of the *RSE* (see Eq. (32)) has to be assessed. Figures 6a,b show samples of the normalized interval displacement field, $w^I(x)E_0J / (p_zL^4)$, pertaining to realizations of the interval Young's modulus $E^I(x)$ with $\hat{e}_i^I = -1$ ($i=1,2,\dots,N=24$) for $l_B = 0.5L$ and two different values of C_B , say $C_B = 0.05$ and $C_B = 0.08$. The FD solution obtained by numerical inversion of the coefficient matrix in Eq.(28), herein labelled as "exact", is contrasted with the approximate solution provided by the *RSE* (see Eq. (32)). The nominal response of the beam with Young's modulus $E(x) = E_0$ is also plotted. It can be seen that the *RSE* approximation is almost coincident with the exact one. Furthermore, as expected, the deviation of the sample of the interval displacement field from the nominal value becomes more appreciable as larger values of the parameter C_B are considered, say as the uncertainty level increases (see Fig. 3). Figure 6 b shows that the *RSE* enables to predict with great accuracy the response of the beam even when large deviations from the nominal solution occur due to Young's modulus fluctuations.

In Fig. 7, the estimates of the UB, LB and midpoint of the normalized interval displacement field, $w^I(x)E_0J/(p_zL^4)$, provided by the approximate explicit expressions in Eqs. (36) and (37) are plotted for $l_b = 0.5L$ and two different values of the parameter C_B , say $C_B = 0.05$ and $C_B = 0.08$. For validation purpose, in Fig. 8 the proposed bounds of the normalized interval displacement field are contrasted with those obtained by applying a combinatorial procedure based on the philosophy of the *vertex method* [4]. Such procedure consists in evaluating the beam response for all possible combinations of the bounds of the *EUIs* \hat{e}_i^I ($i=1,2,\dots,N$) in Eq.(14), say 2^N , and then take at each discretization point x_j of the domain $[0,L]$ the maximum and minimum among all the solutions so obtained. The computational time required by the combinatorial procedure becomes prohibitive even when a small number N of terms is retained in the decomposition (9) of the *spatial dependency function* $\Gamma_b(x,\xi)$. For this reason, numerical results reported in Fig. 8 are obtained assuming $N=16$ instead of $N=24$. By inspection of Fig. 8, it is noted that the proposed explicit expressions (36) of the response bounds provide very accurate estimates of the region of the interval displacement field even when large fluctuations of the uncertain Young's modulus are involved. It is worth emphasizing that unlike the combinatorial procedure, the proposed approach guarantees high computational efficiency also for very refined FD discretizations and a large number of series terms N in Eq. (9). This implies that the closed-form expressions of the interval displacement field can be efficiently exploited to carry out a parametric analysis which is very useful to investigate the effects of Young's modulus uncertainty on the response of the beam. The attention is focused here on the non-probabilistic counterpart of the *coefficient of variation*, say the so-called *coefficient of interval uncertainty* of the response, defined as the ratio $\Delta w(x)/\text{mid}\{w^I(x)\}$ between the deviation amplitude and the midpoint of the interval displacement field. Figure 9a displays the *coefficient of interval uncertainty* of the displacement at two different locations, $x_i = L/2$ and $x_i = L/4$, versus the ratio l_b/L governing the spatial dependency of the interval

Young's modulus field. It is observed that the *coefficient of interval uncertainty* at $x_i = L/4$ is larger than the one at mid-span which implies that the response at quarter span is more affected by the material property uncertainty. Furthermore, as the ratio l_B/L increases, the *coefficient of interval uncertainty* tends to $C_B = 0.05$ which is the value of the ratio $\Delta w(x)/\text{mid}\{w^I(x)\}$ pertaining to the beam with totally spatial dependent Young's modulus field. Indeed, as outlined in Section 3.3, in this case the uncertain elastic modulus is described by an interval variable with deviation amplitude C_B over the whole domain (see Eq. (22)). In Fig. 9b, the *coefficient of interval uncertainty* of the response versus the parameter C_B is plotted. As expected, the coefficient increases linearly with the parameter C_B which governs the deviation amplitude of the interval Young's modulus.

5.3 Fixed-simply supported beam with interval Young's modulus

The fixed-simply supported beam under a deterministic uniformly distributed load p_z shown in Fig.10 is now considered.

The proposed procedure is applied to analyze the response of the beam with uncertain Young's modulus described by an interval field $E^I(x)$ with exponential *spatial dependency function* $\Gamma_B(x, \xi)$. In order to demonstrate the accuracy of the *RSE* (see Eq. (32)), in Figs. 11a,b samples of the normalized interval displacement field, $w^I(x)E_0J/(p_zL^4)$, pertaining to realizations of the interval Young's modulus $E^I(x)$ with $\hat{e}_i^I = +1$ ($i = 1, 2, \dots, N = 24$) for $l_B = 0.5L$ and two different values of C_B , say $C_B = 0.05$ and $C_B = 0.08$, are plotted. The "exact" FD solution, obtained by numerical inversion of the coefficient matrix in Eq.(28), is compared with the *RSE* approximation of the response (see Eq. (32)). For the sake of completeness, the nominal response of the beam with Young's modulus $E(x) = E_0$ is also reported. Notice that the *RSE* allows to capture with great

accuracy the deviation of the sample of the interval displacement field from the nominal value due to Young's modulus uncertainty.

Figure 12 shows the proposed estimates of the UB, LB and midpoint (see Eqs. (36) and (37)) of the normalized interval displacement field, $w^I(x)E_0J/(p_zL^4)$, for $l_B = 0.5L$ and two different values of the parameter C_B , say $C_B = 0.05$ and $C_B = 0.08$. As expected, the region of the response widens as the parameter C_B governing the deviation amplitude of the Young's modulus interval field increases (see Fig. 12b). In Fig. 13, the accuracy of the proposed bounds of the response is demonstrated by comparison with the LB and UB obtained following the philosophy of the *vertex method* [4], say considering the 2^N combinations of the bounds of the *EUIs* \hat{e}_i^I ($i = 1, 2, \dots, N$) in Eq.(14). Notice that the approximate closed-form expressions in Eqs. (36) and (37) provide a very good match with the exact bounds of the interval displacement field even when larger uncertainties are considered. As in the previous example, due to the heavy computational burden associated with the combinatorial procedure, the comparison between the proposed bounds and the exact ones is performed retaining $N = 16$ terms in Eq.(9) instead of $N = 24$.

Finally, the effects of the parameters l_B and C_B characterizing the proposed interval field model $E^I(x)$ with exponential *spatial dependency function* $\Gamma_B(x, \xi)$ are investigated. Figure 14a displays the *coefficient of interval uncertainty* of the displacement, $\Delta w(x)/\text{mid}\{w^I(x)\}$, at two different locations, $x_i = L/2$ and $x_i = L/4$, versus l_B/L . By inspection of Fig. 14a, it can be inferred that the response is much more affected by the material property uncertainty at $x_i = L/4$ than at mid-span. Indeed, the *coefficient of interval uncertainty* at $x_i = L/4$ is much larger than the one at mid-span. Nevertheless, at both locations as the ratio l_B/L increases the *coefficient of interval uncertainty* tends to the value $C_B = 0.05$ pertaining to the beam with totally spatial dependent Young's modulus field. As expected, Fig. 14b shows that the *coefficient of interval uncertainty* of

the response increases linearly with the parameter C_B taking larger values at $x_i = L/4$ than at mid-span.

6. CONCLUSIONS

A non-probabilistic approach for analyzing the effects of Young's modulus uncertainty on the response of Euler-Bernoulli beams under deterministic static loads has been presented. A novel interval field model [17] has been adopted to describe the variability of the uncertain material property along the beam. Such model has been developed in the context of the so-called *improved interval analysis (IIA)*, recently proposed by the authors [7,8] to limit the overestimation affecting the solutions provided by the *classical interval analysis (CIA)* as a result of the *dependency phenomenon*. The key feature of the *IIA* consists in the introduction of an *extra unitary interval (EUI)* able to overcome the main drawbacks of the *CIA*. The novel interval field model accounts for the dependency between interval values of a non-deterministic property at various locations by introducing a deterministic symmetric non-negative bounded function playing the same role of the autocorrelation function in random field theory. Based on the analogy with the random field concept, the interval field has been decomposed as superposition of interval functions by applying a Karhunen-Loève-like expansion in conjunction with the *IIA*. Then, such decomposition has been efficiently exploited in the context of a finite difference discretization of the governing interval ordinary differential equation to derive approximate explicit expressions of the bounds of the interval displacement field along the beam. This remarkable result has been achieved by applying the so-called *Rational Series Expansion (RSE)* [8,22] for evaluating the inverse of the interval coefficient matrix of the discretized equations in approximate closed-form.

The main features of the proposed approach can be summarized as follows: *i*) the capability of accounting for the spatial dependency of uncertain properties within the interval framework by

adopting a novel interval field definition; *ii*) the high computational efficiency due to the possibility of deriving approximate closed-form expressions of the bounds of the interval displacement field after performing a finite difference discretization of the governing interval differential equation.

The proposed approach has been applied to analyze the effects of the interval Young's modulus on the response of both statically determined and indeterminate beams subjected to deterministic static loads. Numerical results have demonstrated the accuracy of the proposed estimates of the bounds of the interval displacement field even for large uncertainty levels. To this aim, appropriate comparisons with the exact solution derived on a combinatorial basis have been performed. The effects of spatial dependency have been thoroughly investigated contrasting the proposed solution with those obtained under the extreme hypotheses of total spatial dependency and spatial independency.

Future research will focus on the extension of the proposed approach to the analysis of two-dimensional problems within a finite element framework.

APPENDIX A

If the real deterministic symmetric non-negative function $\Gamma_B(x, \xi)$ governing the spatial dependency of the interval field is selected so as to have the exponential form reported in Eq. (19), the eigenfunctions solutions of the homogeneous Fredholm integral equation of the second kind (10) are given by [23]:

$$\psi_j(x') = \frac{\cos(\beta_j x')}{\sqrt{l + \frac{\sin(2\beta_j l)}{2\beta_j}}}; \quad \psi_j^*(x') = \frac{\sin(\beta_j^* x')}{\sqrt{l - \frac{\sin(2\beta_j^* l)}{2\beta_j^*}}} \quad (\text{A.1 a,b})$$

where $x' = x - L/2$; $l = L/2$; β_j and β_j^* can be obtained as solutions of the following transcendental equations:

$$c - \tan(\beta l) = 0; \quad \beta^* + c \tan(\beta^* l) = 0 \quad (\text{A.2 a,b})$$

where $c = 1/l_B$.

The eigenvalues associated to the eigenfunctions (A.1 a,b) are given by:

$$\lambda_j = \frac{2C_B^2 c}{\beta_j^2 + c^2}; \quad \lambda_j^* = \frac{2C_B^2 c}{\beta_j^{*2} + c^2}. \quad (\text{A.3 a,b})$$

REFERENCES

- [1] Ben-Haim Y, Elishakoff I. *Convex Models of Uncertainty in Applied Mechanics*. Amsterdam: Elsevier; 1990.
- [2] Moore RE. *Interval Analysis*. Englewood Cliffs: Prentice-Hall; 1966.
- [3] Moore RE, Kearfott RB, Cloud MJ. *Introduction to Interval Analysis*. Philadelphia: SIAM; 2009.
- [4] Moens D, Vandepitte D. A survey of non-probabilistic uncertainty treatment in finite element analysis. *Comput Methods Appl Mech Eng* 2005; 194: 1527–1555.
- [5] Moens D, Hanss M. Non-probabilistic finite element analysis for parametric uncertainty treatment in applied mechanics: Recent advances. *Finite Elem Anal Des* 2011; 47: 4-16.
- [6] Muscolino G, Sofi A. Response statistics of linear structures with uncertain-but-bounded parameters under Gaussian stochastic input. *Int J Struct Stab Dyn* 2011; 11: 775–804.
- [7] Muscolino G, Sofi A. Stochastic analysis of structures with uncertain-but-bounded parameters via improved interval analysis. *Prob Eng Mech* 2012; 28: 152-163.
- [8] Muscolino G, Sofi A. Bounds for the stationary stochastic response of truss structures with uncertain-but-bounded parameters. *Mech Syst Signal Process* 2013; 37: 163-181.

- [9] Hansen ER. A generalized interval arithmetic. In: K. Nicket (Ed.), *Interval Mathematics, Lecture Notes in Computer Science 29*, 7-18. New York: Springer; 1975.
- [10] Comba JLD, Stolfi J. Affine arithmetic and its applications to computer graphics. *Anais do VI Simposio Brasileiro de Computacao Grafica e Processamento de Imagens (SIBGRAPI'93*”, Recife (Brazil), October, 9–18, 1993.
- [11] Nedialkov NS, Kreinovich V, Starks SA. Interval arithmetic, affine arithmetic, Taylor series methods: why, what next? *Numer Algorithms* 2004; 37: 325-336.
- [12] Elishakoff I, Miglis Y. Novel parameterized intervals may lead to sharp bounds. *Mech Res Commun* 2012; 44; 1-8.
- [13] Vanmarcke E. *Random Fields: Analysis and Synthesis*. World Scientific (Revised and Expanded New Edition); 2010
- [14] Moens D, De Munck M, Desmet W, Vandepitte D. Numerical dynamic analysis of uncertain mechanical structures based on interval fields. *IUTAM Symposium on the Vibration Analysis of Structures with Uncertainties (A.K. Belyaev, R.S. Langley eds.)* Springer, Dordrecht 2011; 71-83.
- [15] Verhaeghe W, Desmet W, Vandepitte D, Joris I, Seuntjens P, Moens D. Application of interval fields for uncertainty modelling in a geohydrological case. *Compdyn 2011-3^o ECCOMAS Thematic Conference (M. Papadrakakis, M. Fragiadakis, V.Plevris eds.)* Corfu, Greece, 25-28 May 2011.
- [16] Verhaeghe W, Desmet W, Vandepitte D, Moens, D. Interval fields to represent uncertainty on the output side of a static FE analysis. *Comput Methods Appl Mech Eng* 2013; 260: 50-62.
- [17] Muscolino G, Sofi A, Zingales M. One-dimensional heterogeneous solids with uncertain elastic modulus in presence of long-range interactions: Interval versus stochastic analysis. *Comput Struct* 2013; 122: 217-229.

- [18]Elishakoff I, Ren YJ, Shinozuka M. Some exact solutions for the bending of beams with spatially stochastic stiffness. *Int J Solids Structures* 1995; 32(16): 2315-2327.
- [19]Rollot O, Elishakoff I. Large variation finite element method for beams with stochastic stiffness. *Chaos Solitons Fract* 2003; 17: 749–779.
- [20]Papadopoulos V, Deodatis G, Papadrakakis M. Flexibility-based upper bounds on the response variability of simple beams. *Comput Methods Appl Mech Engrg* 2005; 194: 1385–1404.
- [21]Arwade SR, Deodatis G. Variability response functions for effective material properties. *Prob Eng Mech* 2011; 26: 174-181.
- [22]Muscolino G, Santoro R, Sofi A. Explicit frequency response functions of discretized structures with uncertain parameters. *Comput Struct* 2014; 133: 64–78.
- [23]Ghanem RG, Spanos PD. *Stochastic Finite Elements: A Spectral Approach*. New York: Springer-Verlag; 1991.
- [24]Rohn J. Interval solution of linear interval equations. *Applications of Mathematica* 1990; 35: 220-224.
- [25]Yamazaki F, Shinozuka M, Dasgupta G. Neumann expansion for stochastic finite element analysis. *J Engrg Mech ASCE* 1988; 114(8): 1335–1354.
- [26]Shinozuka M, Deodatis G. Response variability of stochastic finite element systems. *J Engrg Mech ASCE* 1988; 114: 499-519.

Highlights

- The response of Euler-Bernoulli beams with interval Young's modulus is analyzed
- Spatial variability of uncertainty is handled by a novel interval field model
- A finite difference discretization of the interval equilibrium equation is performed
- The bounds of the interval displacement field are evaluated in explicit form
- Numerical results demonstrate both the accuracy and consistency of the proposed model

Figure 1

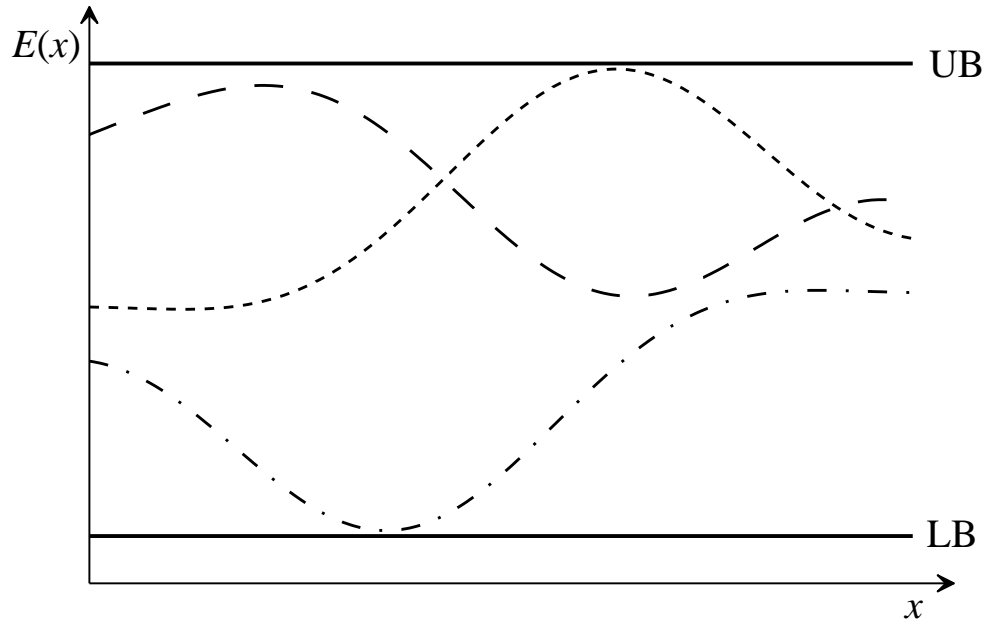


Figure 1. Illustrative representation of the interval field concept.

Figure 2

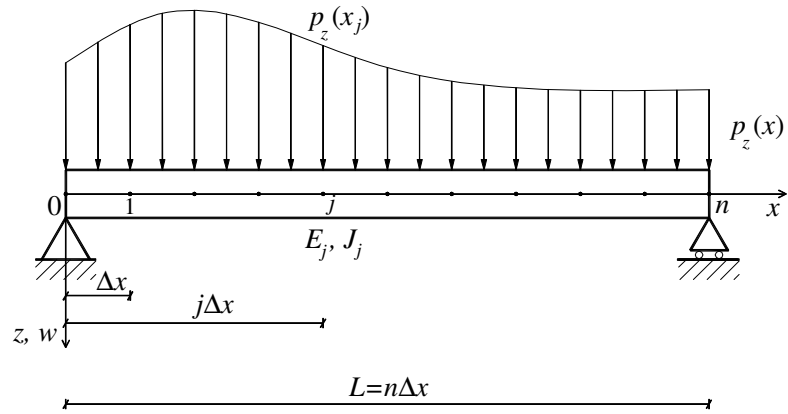


Figure 2. Euler-Bernoulli beam under distributed load.

Figure 3

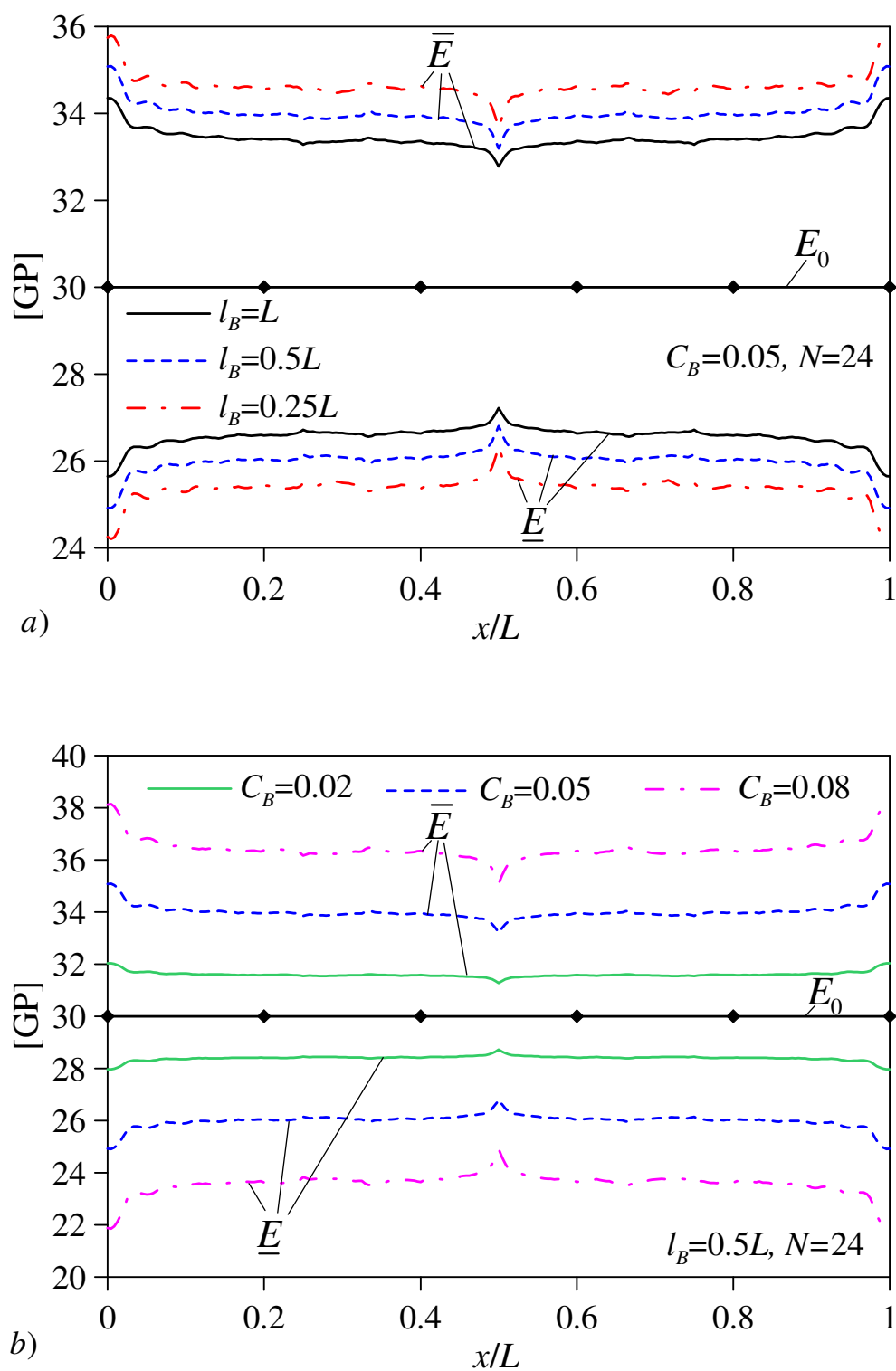


Figure 3. Region of the interval Young's modulus field along the beam for different values of: a) the parameter l_B governing the spatial dependency of the interval field; b) the parameter C_B governing the deviation amplitude of the interval field (see Eq.(22)).

Figure 4

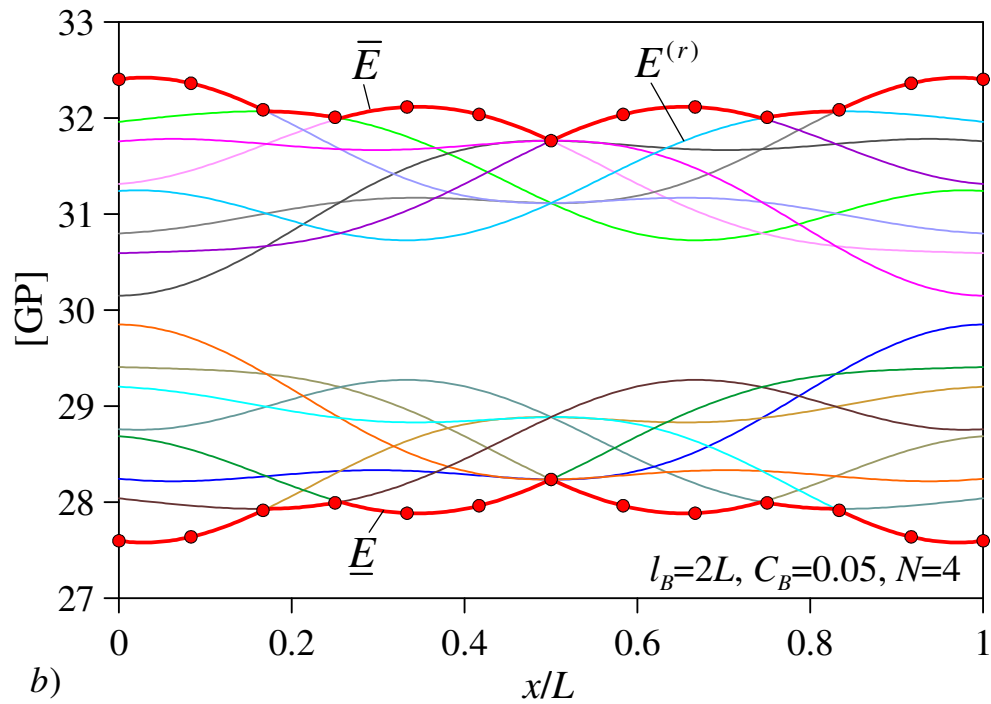
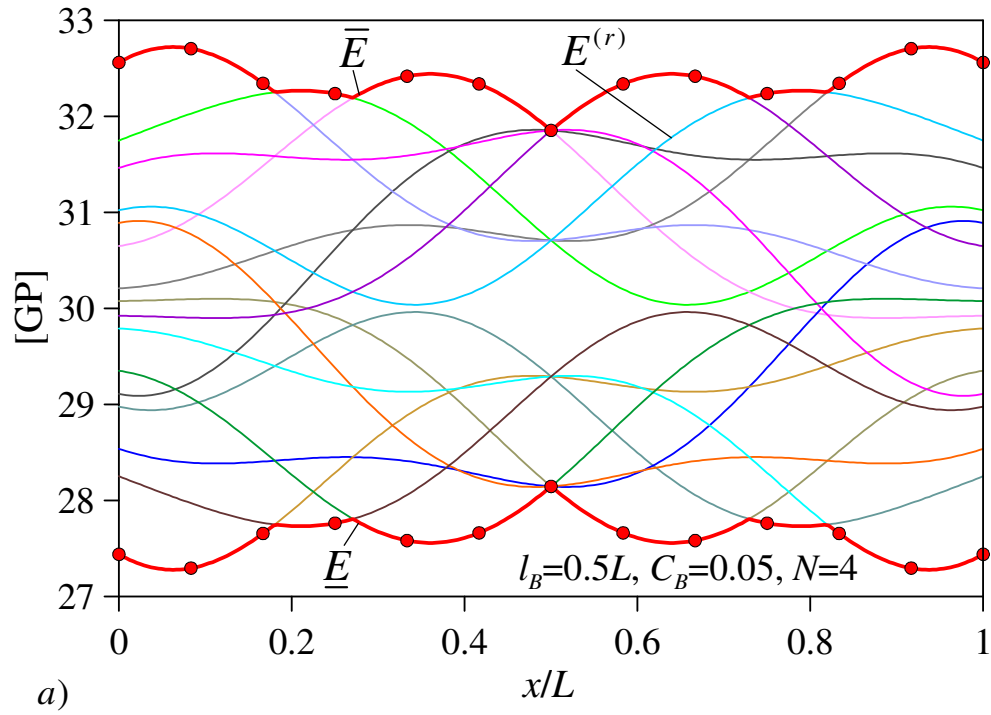


Figure 4. Bounds, \underline{E} and \bar{E} , and samples $E^{(r)}$ ($r=1,2,\dots,2^N$) of the interval Young's modulus field corresponding to all possible combinations of the bounds of the EUIs \hat{e}_i^l , ($i=1,2,\dots,N=4$), (see Eq.(14)).

Figure 5

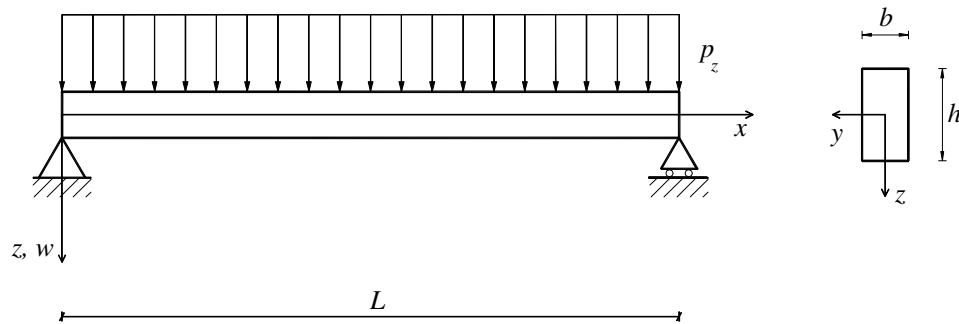


Figure 5. Simply supported beam with interval Young's modulus under uniformly distributed load.

Figure 6

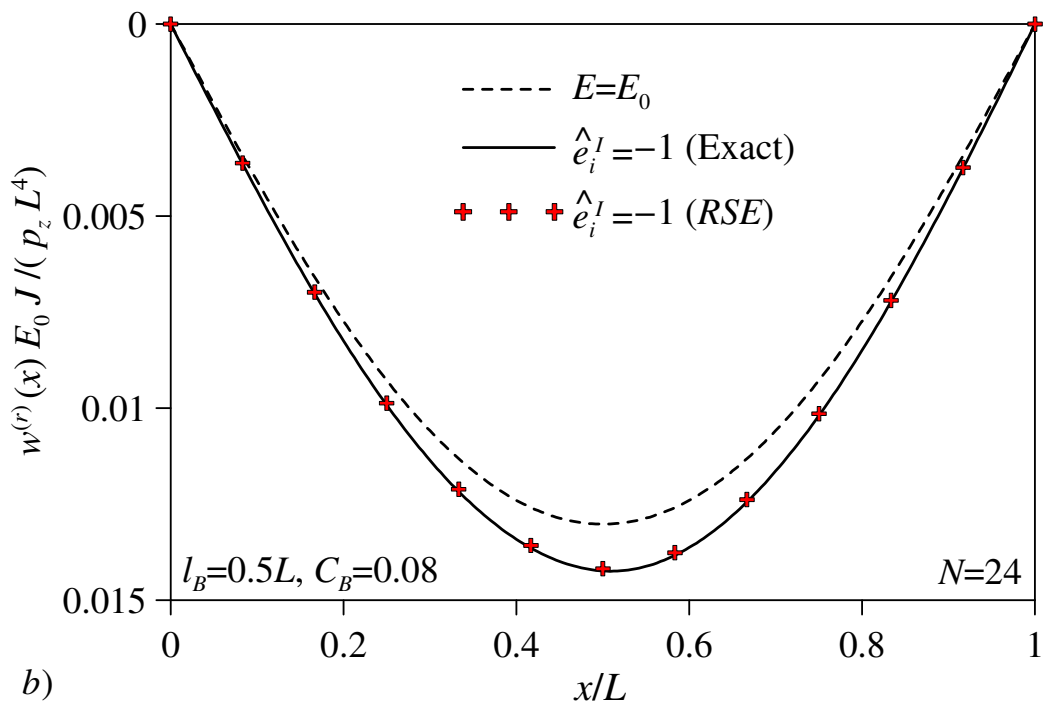
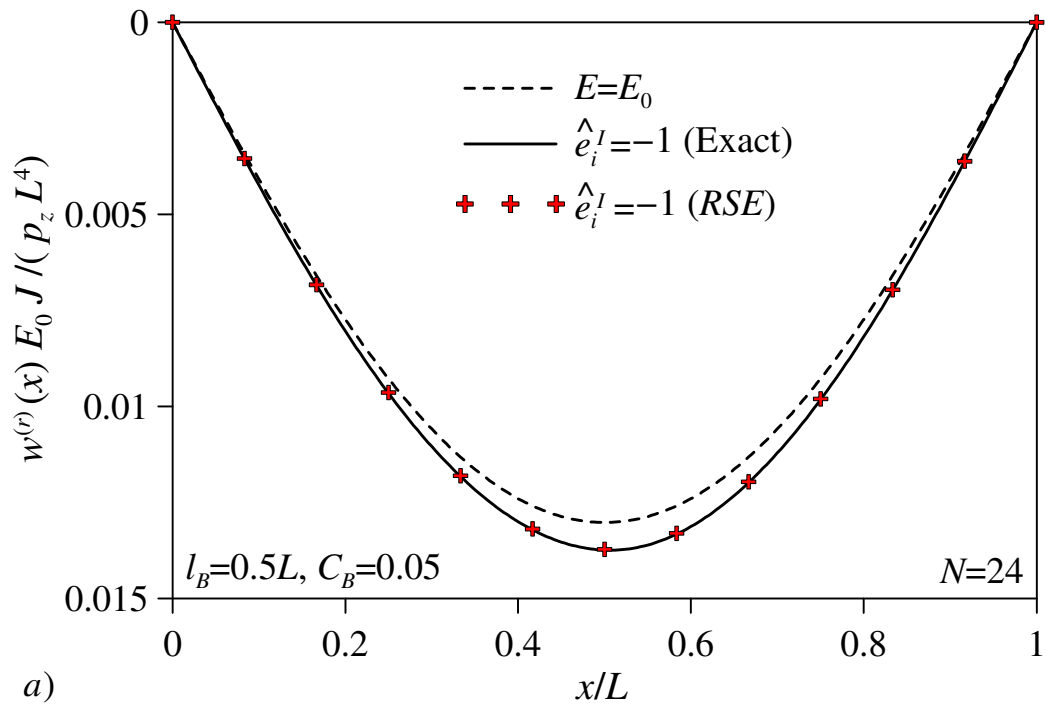


Figure 6. Sample of the normalized interval displacement field along the simply supported beam: comparison between the “exact” FD solution and the *RSE* approximation for a) $C_B = 0.05$ and b) $C_B = 0.08$ ($l_B = 0.5L$).

Figure 7

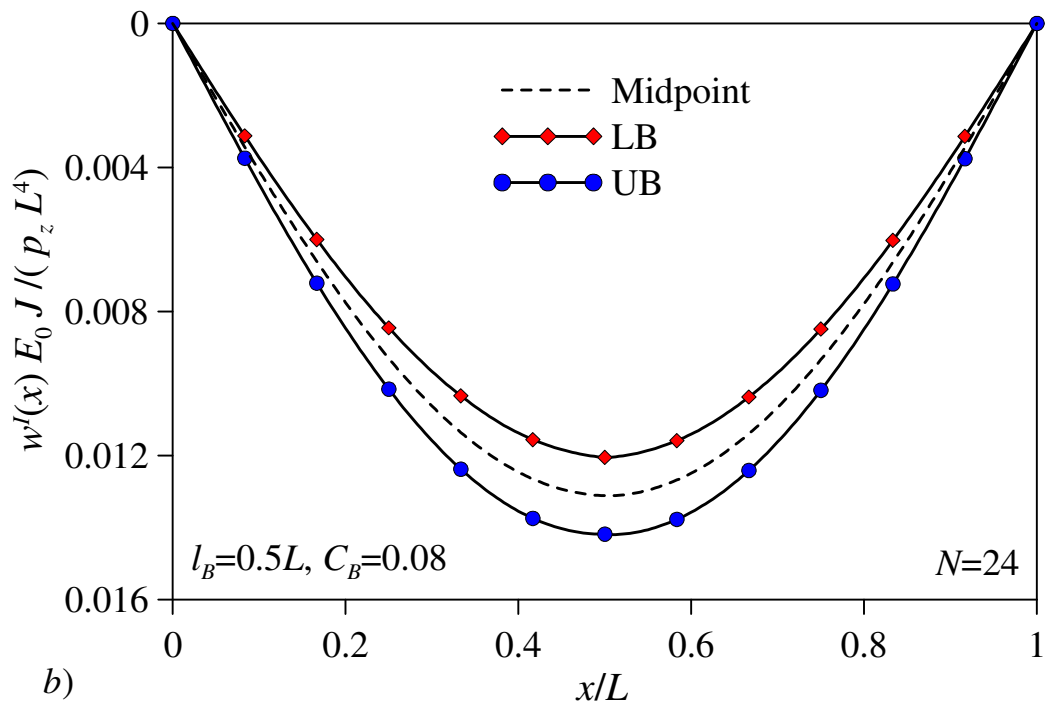
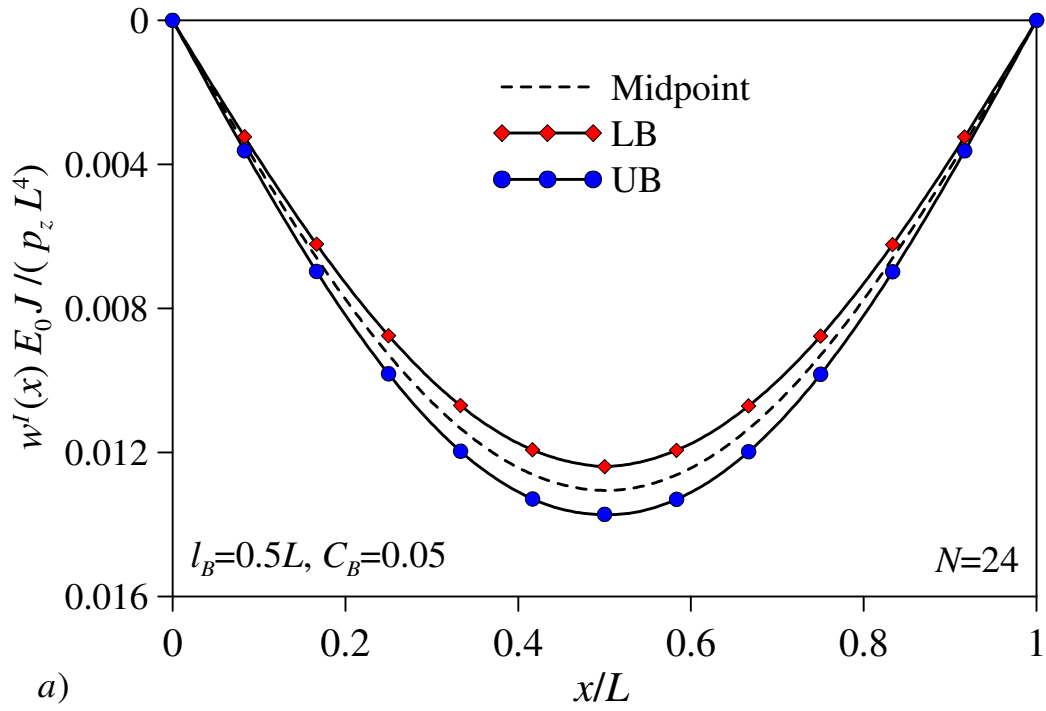


Figure 7. Proposed LB, UB and midpoint of the normalized interval displacement field along the simply supported beam for a) $C_B = 0.05$ and b) $C_B = 0.08$ ($l_B = 0.5L$).

Figure 8

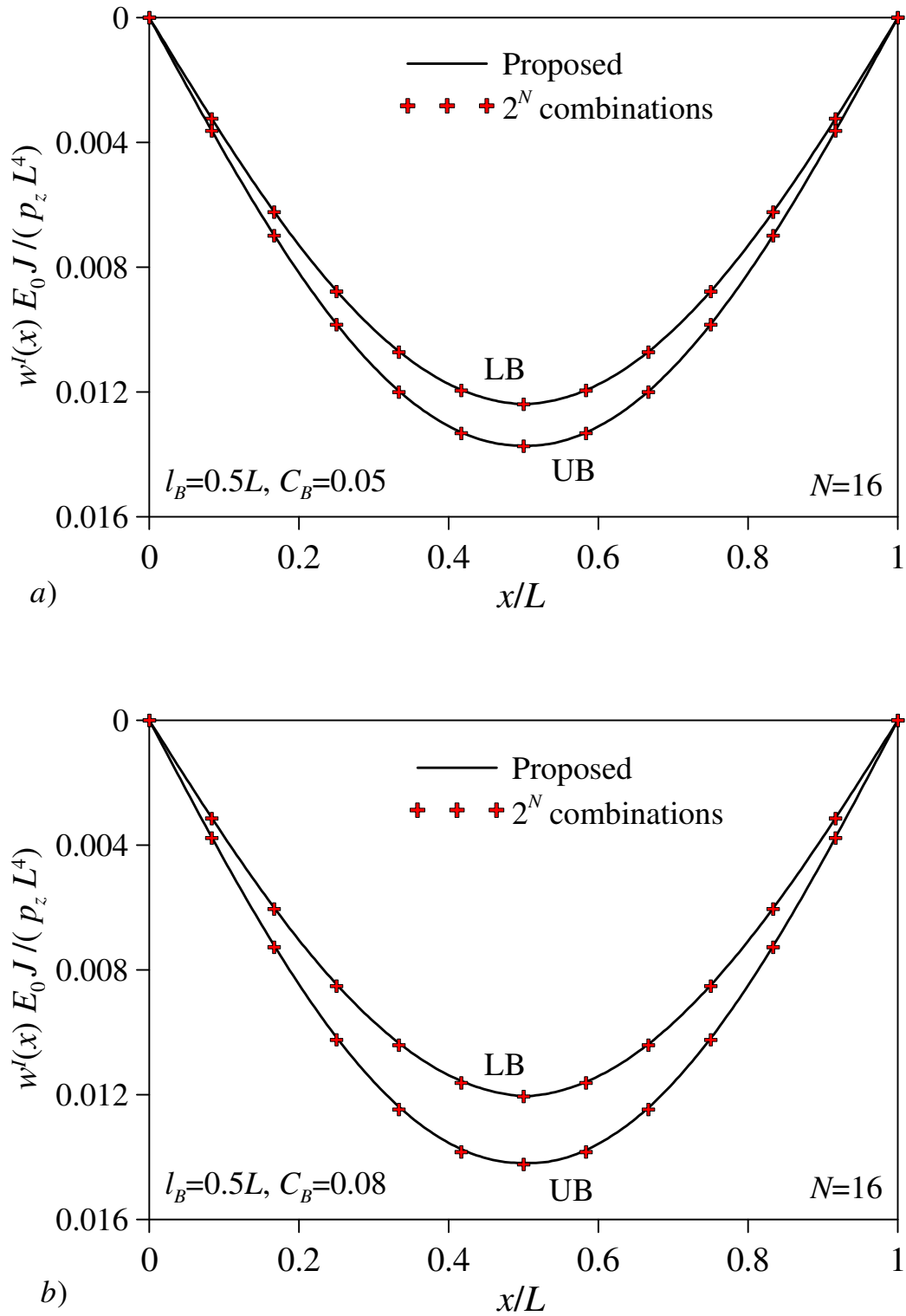


Figure 8. Comparison between the proposed bounds of the normalized interval displacement field along the simply supported beam and the exact ones obtained by a combinatorial procedure for a) $C_B = 0.05$ and b) $C_B = 0.08$ ($l_B = 0.5L$).

Figure 9

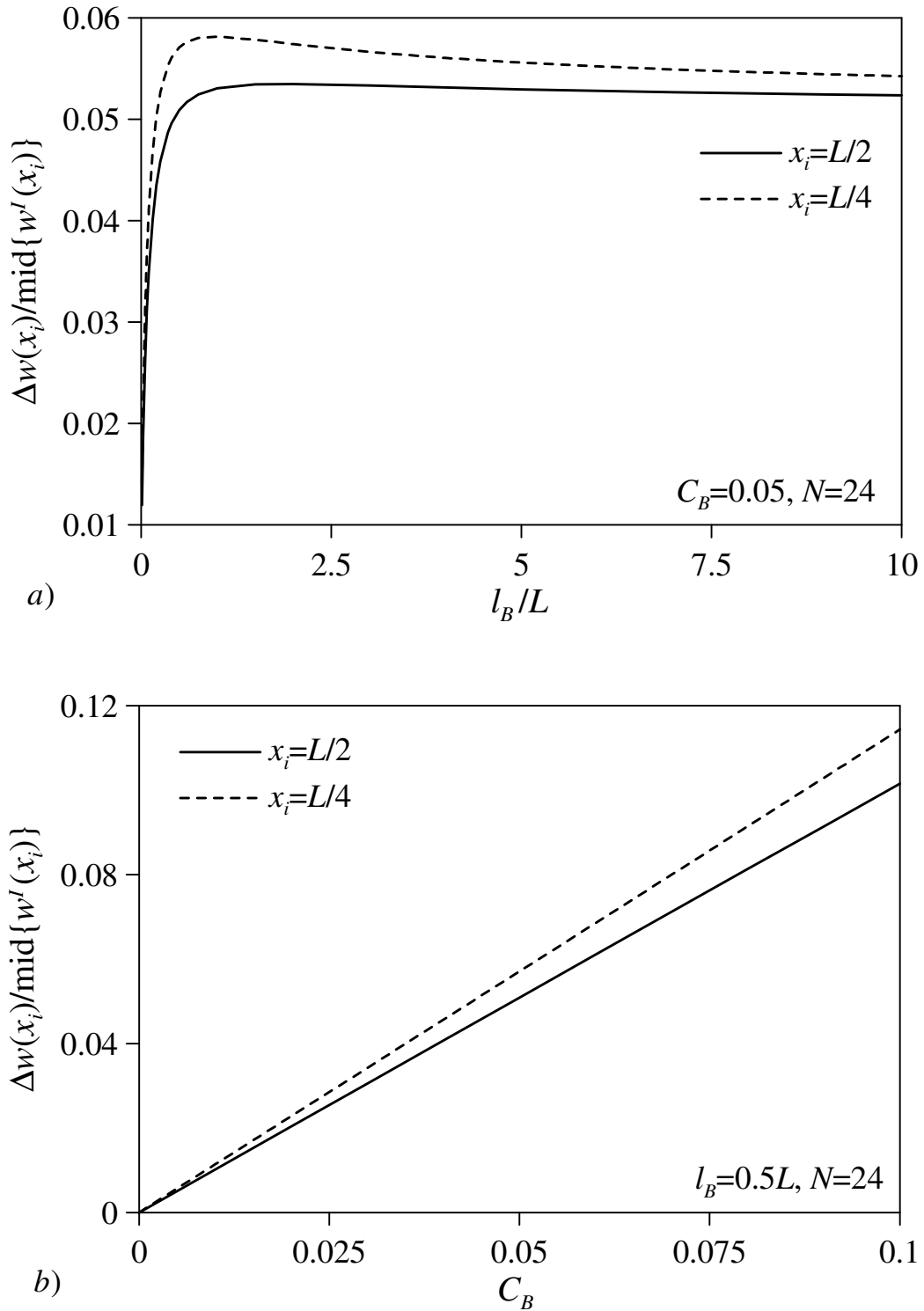


Figure 9. Coefficient of interval uncertainty at the abscissas $x_i = L/2$ and $x_i = L/4$ of the simply supported beam versus: a) the ratio l_B/L and b) the coefficient C_B governing the spatial dependency and deviation amplitude of the interval Young's modulus field, respectively.

Figure 10

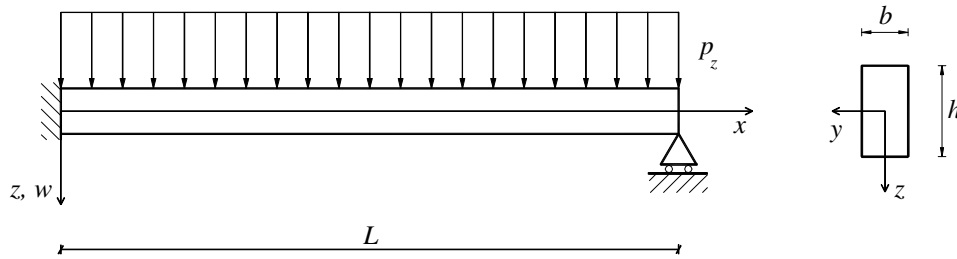


Figure 10. Fixed-simply supported beam with interval Young's modulus under uniformly distributed load.

Figure 11

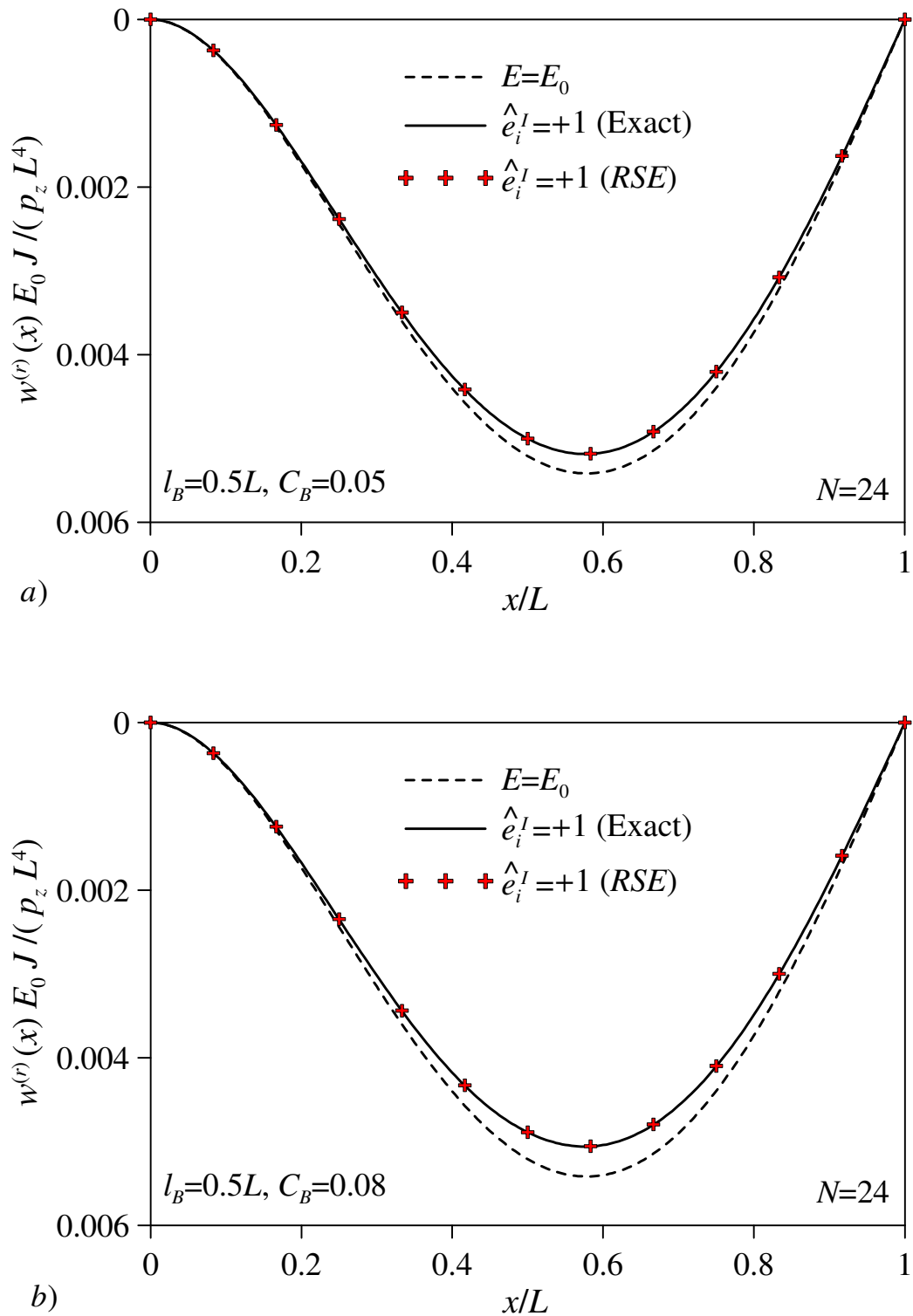


Figure 11. Sample of the normalized interval displacement field along the fixed-simply supported beam: comparison between the “exact” FD solution and the RSE approximation for a) $C_B = 0.05$ and b) $C_B = 0.08$ ($l_B = 0.5L$).

Figure 12

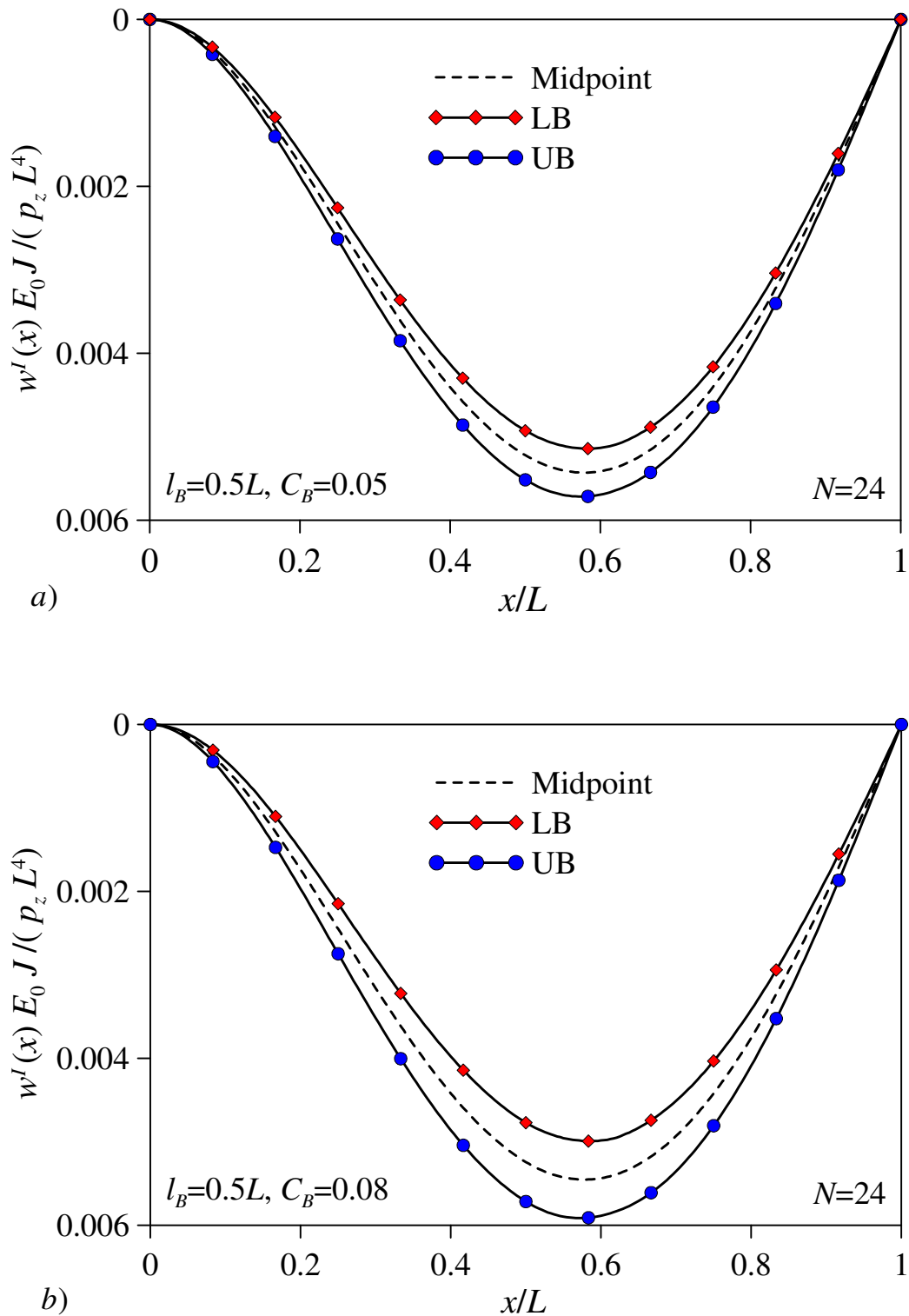


Figure 12. Proposed LB, UB and midpoint of the normalized interval displacement field along the fixed-simply supported beam for a) $C_B = 0.05$ and b) $C_B = 0.08$ ($l_B = 0.5L$).

Figure 13

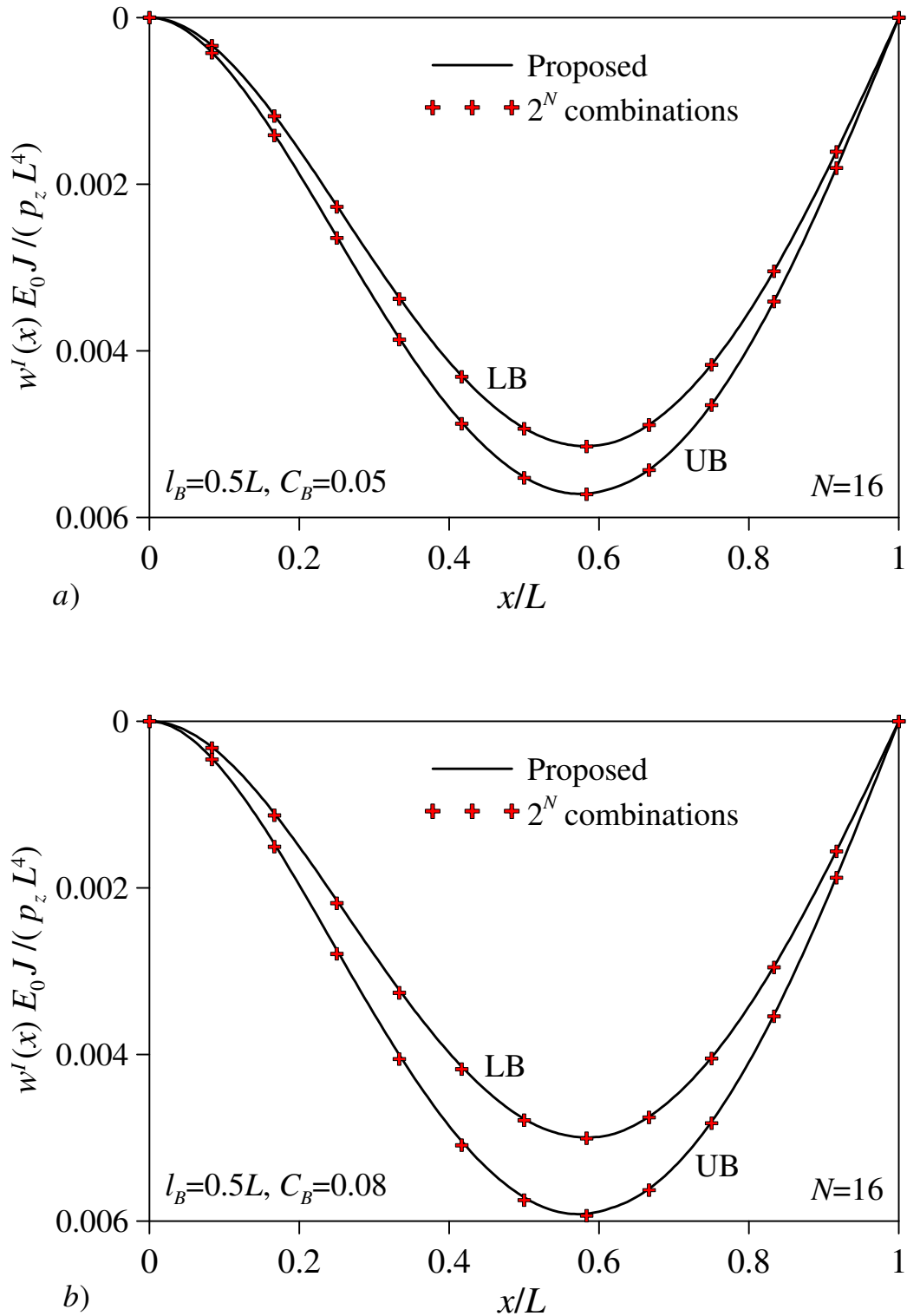


Figure 13. Comparison between the proposed bounds of the normalized interval displacement field along the fixed-simply supported beam and the exact ones obtained by a combinatorial procedure for a) $C_B = 0.05$ and b) $C_B = 0.08$ ($l_B = 0.5L$).

Figure 14

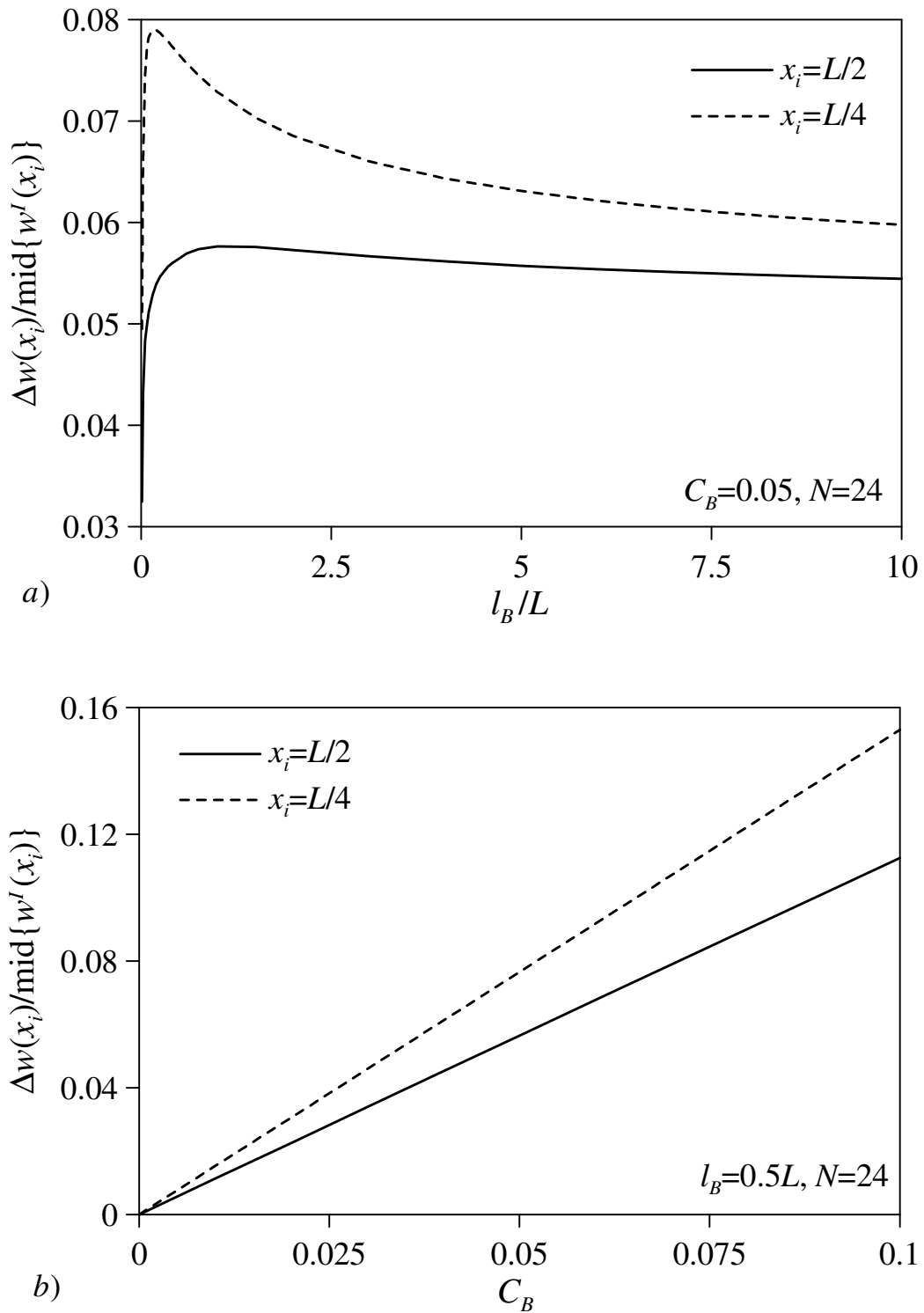


Figure 14. Coefficient of interval uncertainty at the abscissas $x_i = L/2$ and $x_i = L/4$ of the fixed-simply supported beam versus: a) the ratio l_B / L and b) the coefficient C_B governing the spatial dependency and deviation amplitude of the interval Young's modulus field, respectively.